

Phosphorescent Ir(III) complexes with both cyclometalate chromophores and phosphine-silanolate ancillary: concurrent conversion of organosilane to silanolate†

Cite this: *Dalton Trans.*, 2013, **42**, 7111

Fushi Zhang,^{*a} Liduo Wang,^a Shih-Han Chang,^b Kuan-Lin Huang,^b Yun Chi,^{*b} Wen-Yi Hung,^{*c} Chih-Ming Chen,^c Gene-Hsiang Lee^d and Pi-Tai Chou^{*d}

Ir(III) metal complexes with general formula $[(C^{\wedge}N)_2Ir(P^{\wedge}SiO)]$, where $(C^{\wedge}N)H$ is 2-phenylisoquinoline (**1**), 2-phenylpyridine (**2**) or 2-(2,4-difluorophenyl)pyridine (**3**), and $(P^{\wedge}SiO)H$ is an organosilanolate ancillary chelate with either diphenylsilyl (**a**) or dimethylsilyl (**b**) substituent, were synthesized, among which the structure of **3a** was also confirmed using single-crystal X-ray diffraction analyses. These complexes exhibit bright phosphorescence in the region of 489–632 nm in solution at room temperature, showing the first successful example of using organosilanolate as an ancillary chelate. For application, organic light emitting diodes (OLEDs) using phosphors **3a** and **3b** doped in *N,N'*-dicarbazolyl-3,5-benzene (mCP) exhibited a maximum brightness of 50 800 cd m⁻² at 800 mA cm⁻² (12 V) with η_{ext} of 10.1% and a brightness of 45 900 cd m⁻² at 700 mA cm⁻² (14.5 V) with η_{ext} of 10.2%, respectively.

Received 10th October 2012,
Accepted 22nd February 2013

DOI: 10.1039/c3dt32408g

www.rsc.org/dalton

1. Introduction

Over the past two decades, Ir(III) metal-based phosphors have been subject to extensive investigation owing to their potential applications in flat-panel displays and lighting applications.^{1–8} This has led to the successful design of a number of red, green and blue-emitting materials for use in phosphorescent organic light-emitting diodes (OLEDs). These Ir(III) phosphors such as $Ir(ppy)_3$, $ppyH = 2\text{-phenylpyridine}$, in which strong spin-orbit coupling is induced by the heavy Ir(III) metal atom, effectively promote intersystem crossing and afford OLEDs with unprecedented luminescence efficiencies.^{9,10} Moreover, tuning the emission across the whole visible spectrum can be achieved by replacement of ppy cyclometalates with phenyl isoquinoline¹¹ or 2,4-difluorophenylpyridine¹² counterparts for generation of red and blue emission, respectively. The success in the

development of these Ir(III) metal based emitting materials is essential for the realization of highly efficient OLEDs.

Conventionally, the aforementioned homoleptic $Ir(ppy)_3$ or analogues have been synthesized by heating of $Ir(acac)_3$ ($acacH = \text{acetylacetonate}$) with three equiv. of 2-phenylpyridine or chelating heterocyclic aromatics $(C^{\wedge}N)H$ at high temperature.¹³ Alternatively, they can be prepared *via* a stepwise manner, by the formation of dicyclopentadienyl dimer with formula $[(C^{\wedge}N)_2Ir(\mu-Cl)]_2$ *via* treatment of $IrCl_3 \cdot nH_2O$ with two equiv. of $(C^{\wedge}N)H$, followed by addition of the third equiv. of $(C^{\wedge}N)H$ at elevated temperature.¹² In such investigations, scientists also realized that the same dicyclopentadienyl dimer $[(C^{\wedge}N)_2Ir(\mu-Cl)]_2$ readily reacts with chelating anions $(L^{\wedge}X)H$ to afford heteroleptic metal complexes $[(C^{\wedge}N)_2Ir(L^{\wedge}X)]$, with retention of almost all desired photophysical characteristics.^{14,15}

In this respect, suitable anionic $L^{\wedge}X$ chelates included acetylacetonate ($acac$),^{16–18} picolinate (pic) and analogues,^{19–22} carbamate,²³ amidinate,^{24,25} dithiophosphate²⁶ and even 2-pyridyl azolate ($pyaz$) ligands.^{27,28} Furthermore, these heteroleptic complexes retain the major emission characteristics of the parent dicyclopentadienyl fragment $[Ir(C^{\wedge}N)_2]$. Minor alteration on the peak wavelength was also noted, which varied according to the electronic characteristics of the $L^{\wedge}X$ ancillary ligand. For instance, the observed red-shifting of emission λ_{max} follows an order of picolinate < *N*-methylsalicyliminate ~ acetylacetonate, which is proportional to their relative

^aDepartment of Chemistry, Tsinghua University, Beijing 100084, China.
E-mail: zhangfs@mail.tsinghua.edu.cn

^bDepartment of Chemistry, National Tsing Hua University, Hsinchu 30013, Taiwan.
E-mail: ychi@mx.nthu.edu.tw; Tel: +886 3 5712956

^cInstitute of Optoelectronic Sciences, National Taiwan Ocean University, Keelung 202, Taiwan. E-mail: wenhung@mail.ntou.edu.tw

^dDepartment of Chemistry, National Taiwan University, Taipei 10617, Taiwan.
E-mail: chop@ntu.edu.tw

†CCDC reference number 905261. For crystallographic data in CIF or other electronic format see DOI: 10.1039/c3dt32408g

electron donor strengths, resulting in a reduction of the emission energy gap.²⁹ Moreover, electron deficient and/or higher field strength L^X ancillaries, such as imidodiphosphinate³⁰ and pyridyl azolate,^{31,32} and phosphorus-containing chelates, such as benzyl phosphine^{33–37} and phosphine substituted pyrazole,³⁸ are particularly suitable for construction of blue- or even bluish-green-emitting Ir(III) metal phosphors.³⁹

In this contribution, we report a systematic synthesis and characterization of heteroleptic Ir(III) complexes possessing an ancillary chelate (P[^]SiO) that is derived from the hypothetical (2-diphenylphosphinophenyl)dialkylsilanol. We believe that this new class of P[^]SiO chelate, due to the synergy of π -accepting diphenylphosphino unit and electron donating silanolate fragment, should render significantly different properties from those of previously discussed ancillary ligands. For example, its dual accepting/donating character and six-membered ligand–metal bonding capability are expected to exhibit enhanced emission efficiencies and intramolecular π – π stacking, details of which are elaborated in the following sections.

2. Experimental

General procedures

All reactions were performed under nitrogen and solvents were distilled from appropriate drying agents prior to use. Commercially available reagents were used without further purification unless otherwise stated. All reactions were monitored using pre-coated TLC plates (0.20 mm with fluorescent indicator UV254). Mass spectra were obtained on a JEOL SX-102A instrument operating in electron impact (EI) or fast atom bombardment (FAB) mode. ¹H and ¹³C NMR spectra were recorded on a Varian Mercury-400 or an INOVA-500 instrument. Elemental analysis was carried out with a Heraeus CHN-O Rapid Elemental Analyzer. Cyclic voltammetry (CV) measurements were performed using a BAS 100 B/W electrochemical analyzer.

Preparation of (2-bromophenyl)diphenylphosphine

A solution of Pd(PPh₃)₄ (0.10 g, 0.087 mmol), diphenylphosphine (3.7 g, 20 mmol), 1-bromo-2-iodobenzene (2.6 mL, 20 mmol), Et₃N (3.1 mL, 22 mmol) and 50 mL of anhydrous toluene was heated at 80 °C for 12 h under nitrogen. After cooling to RT, the solvent was removed under reduced pressure and washed with deionized water. Further purification was carried out by silica-gel column chromatography eluting with a 1:20 mixture of ethyl acetate–hexane to give a white solid product 6.7 g (17 mmol, 98%).

Selected spectral data. ¹H NMR (400 MHz, CDCl₃, 298 K): δ 7.66–7.63 (m, 1H), 7.38–7.36 (m, 6H), 7.31–7.20 (m, 4H), 7.19–7.21 (m, 2H), 6.75–6.77 (m, 1H).

Preparation of L1 and L2

n-BuLi (2.5 M in hexane, 2.9 mL, 7.3 mmol) was slowly added to a solution of (2-bromophenyl)diphenylphosphine (2.3 g, 6.6 mmol) in 50 mL of THF at –78 °C. The solution was stirred for 30 min at –78 °C before chlorodiphenylsilane (1.5 mL,

7.7 mmol) was added. The resulting mixture was maintained at –78 °C for another 30 min, followed by slowly warming up to RT and then stirred for another 12 h. The solution was concentrated and the precipitate was washed with deionized water, and then recrystallized from CH₂Cl₂–hexanes, giving a colorless solid of (2-diphenylphosphinophenyl)diphenylsilane (L1, 2.0 g, 4.5 mmol, 70%). The analogous (2-diphenylphosphinophenyl)dimethylsilane (L2) was similarly prepared in 90% yield using (2-bromophenyl)diphenylphosphine and chlorodimethylsilane as the starting materials.

Selected spectral data for L1. ¹H NMR (400 MHz, CD₂Cl₂, 298 K): δ 7.51–7.48 (m, 5 H), 7.36–7.22 (m, 15 H), 7.10 (t, $J_{\text{HH}} = 6.0$ Hz, 4 H), 5.82 (d, $J_{\text{PH}} = 6.8$ Hz, Si–H, 1 H). ³¹P NMR (202 MHz, acetone-d₆, 298 K): δ –9.72 (s, 1 P).

Selected spectral data for L2. ¹H NMR (400 MHz, CD₂Cl₂, 298 K): δ 7.66–7.63 (m, 1 H), 7.35–7.30 (m, 8 H), 7.26–7.22 (m, 4 H), 7.10–7.07 (m, 1 H), 4.71–4.65 (m, Si–H), 0.36 (dd, $J_{\text{HH}} = 3.6$ Hz, $J_{\text{PH}} = 1.2$ Hz, 2 CH₃, 6 H). ³¹P NMR (202 MHz, acetone-d₆, 298 K): δ –9.94 (s, 1 P).

Synthesis of [(piq)₂Ir(L1)] (1a)

All cyclometalated Ir(III) complexes were synthesized by the generalized protocol as indicated in the literature.^{40,41} A typical procedure is given below.

A solution of [(piq)₂Ir(μ -Cl)]₂ (500 mg, 0.39 mmol), L1 (380 mg, 0.86 mmol), Na₂CO₃ (410 mg, 3.9 mmol) and 2-methoxyethanol (10 mL) was heated at 120 °C for 2 h. After cooling to RT, the solvent was removed under reduced pressure and the residue was purified by silica-gel column chromatography eluting with a 1:1 mixture of ethyl acetate and hexanes. Recrystallization from ethyl acetate–hexanes gave a red crystalline solid (1a, 530 mg, 0.50 mmol, 64%).

Selected spectral data for 1a. ¹H NMR (400 MHz, CD₂Cl₂, 298 K): δ 9.31 (d, $J_{\text{HH}} = 6.8$ Hz, 1 H), 8.82 (d, $J_{\text{HH}} = 8.4$ Hz, 1 H), 8.74 (d, $J_{\text{HH}} = 6.4$ Hz, 1 H), 8.63 (d, $J_{\text{HH}} = 8.4$ Hz, 1 H), 8.11 (d, $J_{\text{HH}} = 7.6$ Hz, 1 H), 7.88 (t, $J_{\text{HH}} = 7.6$ Hz, 2 H), 7.72–7.64 (m, 5 H), 7.61–7.55 (m, 3 H), 7.48 (t, $J_{\text{HH}} = 8.4$, 2 H), 7.40 (t, $J_{\text{HH}} = 7.6$ Hz, 1 H), 7.33–7.24 (m, 5 H), 7.19–7.08 (m, 4 H), 6.95–6.87 (m, 2 H), 6.80–6.69 (m, 5 H), 6.62–6.56 (m, 2 H), 6.49–6.37 (m, 6 H), 6.30 (d, $J_{\text{HH}} = 7.6$ Hz, 1 H), 6.03 (m, 1 H); ³¹P NMR (202 MHz, CD₂Cl₂, 298 K): δ –0.57 (s, 1 P); MS (FAB, ¹⁹³Ir): m/z : 1060 [M]⁺. Anal. Calc. for C₆₀H₄₄IrN₂OPSi: N, 2.64; C, 67.96; H, 2.68. Found: N, 2.84; C, 68.15; H, 2.52%.

Synthesis of [(ppy)₂Ir(L1)] (2a)

Yield: 31%. Selected spectral data: ¹H NMR (400 MHz, acetone-d₆, 298 K): δ 9.19 (d, $J_{\text{HH}} = 5.6$ Hz, 1 H), 8.86 (d, $J_{\text{HH}} = 6$ Hz, 1 H), 7.89 (d, $J_{\text{HH}} = 8$ Hz, 1 H), 7.78–7.72 (m, 2 H), 7.56–7.55 (m, 4 H), 7.49–7.45 (m, 4 H), 7.40–7.29 (m, 3 H), 7.22–7.14 (m, 6 H), 7.08–7.01 (m, 2 H), 6.88–6.72 (m, 8 H), 6.65–6.58 (m, 4 H), 6.45 (t, $J_{\text{HH}} = 8.4$ Hz, 2 H), 6.33 (d, $J_{\text{HH}} = 6.4$ Hz, 1 H), 5.88 (m, 1 H); ³¹P NMR (202 MHz, CD₂Cl₂, 298 K): δ 0.69 (s, 1 P); MS (FAB, ¹⁹³Ir): m/z : 962 [M]⁺. Anal. Calc. for C₅₂H₄₂IrN₂OPSi: N, 2.91; C, 64.91; H, 4.40. Found: N, 2.78; C, 65.03; H, 4.14%.

Synthesis of [(dfppy)₂Ir(L1)] (3a)

Yield: 70%. Selected spectral data: ¹H NMR (400 MHz, CD₂Cl₂, 298 K): δ 9.06 (d, *J*_{HH} = 5.2 Hz, 1 H), 8.81 (d, *J*_{HH} = 6.0 Hz, 1 H), 8.07 (d, *J*_{HH} = 6.4 Hz, 1 H), 7.74–7.64 (m, 3 H), 7.49–7.35 (m, 7 H), 7.29–7.23 (m, 8 H), 7.16–7.05 (m, 2 H), 6.92–6.76 (m, 7 H), 6.54 (t, *J*_{HH} = 6.4 Hz, 1 H), 6.46 (t, *J*_{HH} = 8.4 Hz, 2 H), 6.33 (m, 1 H), 6.21 (m, 1 H), 5.71 (dd, *J*_{HH} = 9.2, 2.0 Hz, 1 H); ¹⁹F {¹H} NMR (376 MHz, CD₂Cl₂, 298 K): δ –106.79 (t, *J* = 8.8 Hz, 1 F), –108.44 (d, *J* = 9.8 Hz, 1 F), –108.81 (t, *J* = 9.4 Hz, 1 F), –109.02 (d, *J* = 10.2 Hz, 1 F); ³¹P NMR (202 MHz, CD₂Cl₂, 298 K): δ –0.01 (t, *J*_{PF} = 8.1 Hz, 1 P); MS (FAB, ¹⁹³Ir): *m/z*: 1032 [M]⁺. Anal. Calc. for C₅₂H₃₆F₄IrN₂OPSi·0.5CH₂Cl₂: N, 2.59; C, 58.91; H, 3.45. Found: N, 2.92; C, 58.76; H, 3.87%.

Synthesis of [(piq)₂Ir(L2)] (1b)

Yield: 61%. Selected spectral data: ¹H NMR (400 MHz, CD₂Cl₂, 298 K): δ 8.90 (q, *J*_{HH} = 8.0 Hz, 3 H), 8.79 (d, *J*_{HH} = 6.4 Hz, 1 H), 8.16 (t, *J*_{HH} = 6.8 Hz, 2 H), 7.85–7.82 (m, 2 H), 7.74–7.68 (m, 4 H), 7.51–7.47 (m, 3 H), 7.38 (m, 1 H), 7.31 (m, 1 H), 7.20–7.14 (m, 3 H), 7.00–6.96 (m, 4 H), 6.89 (t, *J*_{HH} = 8 Hz, 1 H), 6.79 (t, *J*_{HH} = 7.6 Hz, 1 H), 6.67 (q, *J*_{HH} = 6.8, 2 H), 6.60–6.52 (m, 3 H), 6.45 (t, *J*_{HH} = 7.2 Hz, 2 H), 5.91–5.89 (m, 1 H), 0.32 (s, 3 H), –0.79 (s, 3 H); ³¹P NMR (202 MHz, CD₂Cl₂, 298 K): δ –0.99 (s, 1P); MS (FAB, ¹⁹³Ir): *m/z*: 937 [M]⁺. Anal. Calc. for C₅₀H₄₀IrN₂OPSi·0.5CH₂Cl₂: N, 2.86; C, 61.98; H, 4.22. Found: N, 2.85; C, 61.86; H, 4.52%.

Synthesis of [(ppy)₂Ir(L2)] (2b)

Yield: 34%. Selected spectral data: ¹H NMR (400 MHz, CD₂Cl₂, 298 K): δ 8.82 (d, *J*_{HH} = 5.2 Hz, 1 H), 8.65 (d, *J*_{HH} = 5.6 Hz, 1 H), 7.93 (d, *J*_{HH} = 7.6 Hz, 1 H), 7.73–7.63 (m, 3 H), 7.56 (t, *J*_{HH} = 7.6 Hz, 1 H), 7.51–7.43 (m, 4 H), 7.37 (t, *J*_{HH} = 6 Hz, 1 H), 7.30 (t, *J*_{HH} = 7.2 Hz, 1 H), 7.16 (t, *J*_{HH} = 7.6 Hz, 4 H), 6.94–6.81 (m, 4 H), 6.73–6.50 (m, 8 H), 5.75–5.72 (m, 1 H), 0.28 (s, 3 H), –0.69 (s, 3 H); ³¹P NMR (202 MHz, CD₂Cl₂, 298 K): δ 0.64 (s, 1 P); MS (FAB, ¹⁹³Ir): *m/z*: 837 [M]⁺. Anal. Calc. for C₅₂H₄₀IrN₂OPSi: N, 3.35; C, 60.34; H, 4.34. Found: N, 3.65; C, 60.12; H, 4.63%.

Synthesis of [(dfppy)₂Ir(L2)] (3b)

Yield: 75%. Selected spectral data: ¹H NMR (400 MHz, CD₂Cl₂, 298 K): δ 8.82 (d, *J*_{HH} = 5.2 Hz, 1 H), 8.65 (d, *J*_{HH} = 6 Hz, 1 H), 8.33 (m, 1 H), 8.09 (d, *J*_{HH} = 8.4 Hz, 1 H), 7.74 (t, *J*_{HH} = 8 Hz, 1 H), 7.62 (t, *J*_{HH} = 7.2 Hz, 1 H), 7.51–7.48 (m, 1 H), 7.44–7.35 (m, 4 H), 7.25–7.16 (m, 4 H), 6.93 (td, *J*_{HH} = 7.6, 2.0 Hz, 2 H), 6.84 (t, *J*_{HH} = 8.4 Hz, 1 H), 6.70 (m, 1 H), 6.64 (m, 1 H), 6.54 (t, *J*_{HH} = 9.2 Hz, 2 H), 6.44–6.38 (m, 1 H), 6.26–6.20 (m, 1 H), 6.00 (dd, *J*_{HH} = 9.2, 2.4 Hz, 1 H), 5.21–5.17 (m, 1 H), 0.29 (s, 3 H), –0.68 (s, 3 H); ¹⁹F {¹H} NMR (376 MHz, CD₂Cl₂, 298 K): δ –107.86 (dd, *J* = 9.8 and 7.9 Hz, 1 F), –109.80 (t, *J* = 9.8 Hz, 1 F), –110.07 (d, *J* = 9.8 Hz, 1 F), –110.62 (d, *J* = 10.2 Hz, 1 F); ³¹P NMR (202 MHz, CD₂Cl₂, 298 K): δ –0.25 (t, *J*_{PF} = 8.1 Hz, 1 P); MS (FAB, ¹⁹³Ir): *m/z*: 909 [M]⁺. Anal. Calc. for C₄₂H₃₂F₄IrN₂OPSi: N, 3.09; C, 55.56; H, 3.55. Found: N, 3.35; C, 55.32; H, 3.64%.

Single-crystal X-ray diffraction studies

Single-crystal X-ray diffraction data were acquired with a Bruker SMART Apex CCD diffractometer using Mo-Kα radiation ($\lambda = 0.71073 \text{ \AA}$). The data collection was executed using the SMART program. Cell refinement and data reduction were performed with the SAINT program. The structure was determined using the SHELXTL/PC program and refined using full-matrix least squares.

Selected crystal data of 3a. C_{52.5}H₃₇ClF₄IrN₂OPSi; *M* = 1074.55; monoclinic, space group = *P*₂₁/*n*; *a* = 14.2505(10), *b* = 14.8900(11), *c* = 21.0030(16) Å, $\beta = 107.351(2)^\circ$, *V* = 4253.8(5) Å³; *Z* = 4; *D*_c = 1.678 Mg m^{–3}; *F*(000) = 2132; crystal size = 0.32 × 0.25 × 0.20 mm³; $\lambda(\text{Mo-K}\alpha) = 0.71073 \text{ \AA}$; *T* = 150(2) K; $\mu = 3.329 \text{ mm}^{-1}$; 32 447 reflections collected, 9764 independent reflections (*R*_{int} = 0.0410), GOF = 1.065, final *R*₁ [*I* > 2σ(*I*)] = 0.0301 and w*R*₂(all data) = 0.0647.

OLED device fabrication

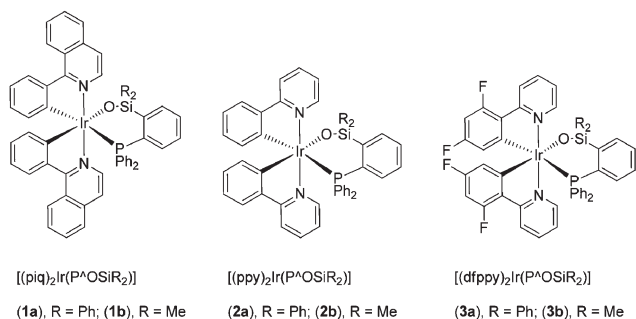
All chemicals were purified through vacuum sublimation prior to use. The OLEDs were fabricated through vacuum deposition of the materials at 10^{–6} torr onto ITO-coated glass substrates having a sheet resistance of 15 Ω sq^{–1}. The ITO surface was sequentially cleaned with acetone, methanol and deionized water, followed by UV-ozone treatment. The deposition rate of each organic material was *ca.* 1–2 Å s^{–1}. Subsequently, LiF was deposited at 0.1 Å s^{–1} and then capped with Al (*ca.* 5 Å s^{–1}) through shadow masking without breaking the vacuum. The *J*–*V*–*L* characteristics of the devices were measured simultaneously in a glove-box using a Keithley 6430 source meter and a Keithley 6487 picoammeter equipped with a calibration Si-photodiode. EL spectra were measured using a photodiode array (Ocean Optics USB2000).

Results and discussion

Synthesis and characterization

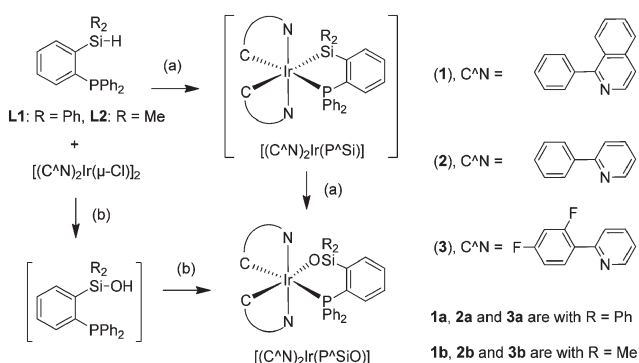
First, (2-diphenylphosphinophenyl)diphenylsilane (**L1**) and (2-diphenylphosphinophenyl)dimethylsilane (**L2**) were synthesized and employed as precursors for the ancillary (P⁺SiO) chelate. These silane reagents were easily obtained from initial lithiation of (2-bromophenyl)diphenylphosphine at –78 °C, followed by addition of either chlorodiphenylsilane or chlorodimethylsilane for inducing the formation of the C–Si bond. In the meantime, the chloride bridged dimers [(C[^]N)₂Ir(μ-Cl)]₂, where (C[^]N)H is 1-phenylisoquinoline (piqH), 2-phenylpyridine (ppyH) or 4,6-difluorophenylpyridine (dfppyH), were routinely synthesized from condensation of IrCl₃·hydrate with two equiv. of (C[^]N)H at elevated temperature. Subsequent treatment of [(C[^]N)₂Ir(μ-Cl)]₂ with the aforementioned organosilane precursors in the presence of Na₂CO₃ and in refluxing methoxyethanol gave the heteroleptic Ir(III) complexes [(C[^]N)₂Ir(P⁺SiO)] (1–3) in moderate yields. Structural drawings of 1–3 are depicted in Scheme 1.

It is notable that, all reactions between [(C[^]N)₂Ir(μ-Cl)]₂ and the dialkylsilane **L1** (or **L2**) have never afforded the Ir(III)



Scheme 1 Structural drawings of the heteroleptic Ir(III) complexes $[(\text{C}^{\wedge}\text{N})_2\text{Ir}(\text{P}^*\text{SiO})]$ (**1–3**).

complexes with the proposed P–Si chelate *via* direct Si–H bond activation, as shown in the proposed structure of $[(\text{C}^{\wedge}\text{N})_2\text{Ir}(\text{P}^*\text{Si})]$ depicted in transformation (a) of Scheme 2. Instead, the $[(\text{C}^{\wedge}\text{N})_2\text{Ir}(\text{P}^*\text{Si})]$ intermediate may be extremely unstable and undergo instant oxidation under the reaction conditions to afford the silanolate complexes of formula $[(\text{C}^{\wedge}\text{N})_2\text{Ir}(\text{P}^*\text{SiO})]$. Such a possibility is demonstrated by the recent reactivity study of a dimethylplatinum(II) complex with the bis-(2-pyridyl)dimethylsilane ligand, for which the cleavage of Si–Me bond and formation of chelating Si–O–Pt linkage are induced by both metal oxidation and hydroxide attack at the silicon atom.⁴² Alternatively, the added organosilane may first convert to free organosilanol during the reaction, for which similar hydrolytic oxidation of organosilanes to the organosilanol had been documented in high yields in the presence of iridium catalysts and under mild conditions.⁴³ The organosilanol then coupled with the added Ir(III) metal reagent $[(\text{C}^{\wedge}\text{N})_2\text{Ir}(\mu\text{-Cl})_2]$ to afford the isolated silanolate complexes $[(\text{C}^{\wedge}\text{N})_2\text{Ir}(\text{P}^*\text{SiO})]$, see transformation (b) shown in Scheme 2. To demonstrate the wide scope of the present method, we also performed syntheses under several distinctive conditions, and the corresponding silanolate products were all obtained in moderate to good yields, particularly for those utilizing “wet” methoxyethanol as the reaction medium. Thus, the current procedure represents an efficient method for the formation of silanolate metal complexes from organosilane reagents.



Scheme 2 Two proposed transformation pathways leading to the Ir(III) complexes $[(\text{C}^{\wedge}\text{N})_2\text{Ir}(\text{P}^*\text{SiO})]$; employed conditions: Na_2CO_3 , methoxyethanol, 120 °C, 2 h.

Despite the fact that we could not obtain the intended Ir(III) complexes with a chelating Ir–Si⁺P unit, complexes with a direct Ir–Si linkage have been documented in literature. Among these investigations, Eisenberg prepared the mono- and bis-silyl complexes of the formula $\text{IrH}_2(\text{SiR}_3)(\text{CO})(\text{dppe})$ and $\text{IrH}(\text{SiR}_3)_2(\text{CO})(\text{dppe})$ ($\text{dppe} = 1,2\text{-bis}(\text{diphenylphosphino})\text{-ethane}$) *via* reaction of $\text{IrH}_3(\text{CO})(\text{dppe})$ with silane reagents (HSiR_3);⁴⁴ Tilley and co-workers reported the isolation of Ir(III) complexes $\text{Cp}^*(\text{PMe}_3)\text{Ir}(\text{SiR}_2\text{OTf})\text{Me}$ ($\text{Cp}^* = \eta^5\text{-C}_5\text{Me}_5$, $\text{OTf} = \text{OSO}_2\text{CF}_3$) *via* activation of silanes (HSiR_3) with $\text{Cp}^*(\text{PMe}_3)\text{Ir}(\text{Me})\text{OTf}$;⁴⁵ also, Milstein reported the formation of the transient silane derivative $(\text{PMe}_3)_3\text{Ir}(\text{SiMe}_2\text{Ph})$ and subsequent Ir(III) iridasilacycle from treatment of $\text{Ir}(\text{PMe}_3)_4\text{Cl}$ and PhMe_2SiLi at ambient temperature.⁴⁶ However, all these reactions were conducted under strictly anaerobic and anhydrous conditions to prevent the possible oxygenation of the silane product, which may explain our failure in obtaining the originally intended Ir–Si complexes. On the other hand, the catalytically active $\{[\text{Ir}(\text{cod})(\mu\text{-OSiMe}_3)]_2\}$ has been synthesized by halide–silanoxide metathesis,⁴⁷ but there is no precedent for the respective Ir(III) silanolate complexes, making our report the first successful case to show their existence and structural characteristics.

Moreover, the photophysical properties of this class of $[(\text{C}^{\wedge}\text{N})_2\text{Ir}(\text{P}^*\text{SiO})]$ complexes, to a certain extent, are analogous to the Ir(III) complexes that possess similar C⁺N chromophores, despite the possession of the third, non-emissive silanolate ancillaries. These properties are elaborated in the following section of photophysical measurement. In addition, all P⁺SiO complexes **1–3** are highly soluble in chlorinated solvents and show negligible decomposition upon raising temperature for both SiPh₂ and SiMe₂ derivatives, *i.e.* either complexes **a** or **b**. Full characterizations were executed using FAB MS spectrometry, NMR techniques and elemental analyses (see Experimental section), while dfppy complex **3a** was further identified by single-crystal X-ray analysis to establish their structure and packing in solid state.

According to the X-ray structural determination, complex **3a** reveals a typical heteroleptic arrangement, with two dfppy cyclometalates and one PPh₂ substituted silanolate ancillary (Fig. 1, also see Scheme 1 for the drawing). The dfppy chelates adopt a mutually eclipsed configuration with their coordinated nitrogen atoms N(1) and N(2) and carbon atoms C(1) and C(12) being located in *trans*- and *cis*-orientation, respectively. Moreover, the P⁺SiO ancillary resides opposite to the carbon atoms of both dfppy chelates. The overall ligand arrangement around the Ir(III) metal center is akin to that of Ir(III) metal complexes with relevant oxygenate ancillaries such as 2-(2-hydroxyphenyl)-substituted benzothiazole and benzoxazole.^{48,49} This suggests that the employed P⁺SiO chelate is capable of coordinating to the Ir(III) metal atom *via* a stereo-selective replacement of chloride ligands in its dinuclear precursor $[(\text{dfppy})_2\text{Ir}(\mu\text{-Cl})_2]$.⁵⁰ Moreover, the elongated Ir–C(1) distance (2.038(3) Å) vs. Ir–C(12) bond (1.995(3) Å) in **3a** also shows a notable *trans*-effect imposed by the strong π-accepting PPh₂ fragment. In fact, the Ir(III) metal complexes with the analogous PPh₂ substituted phenolate chelate also show the

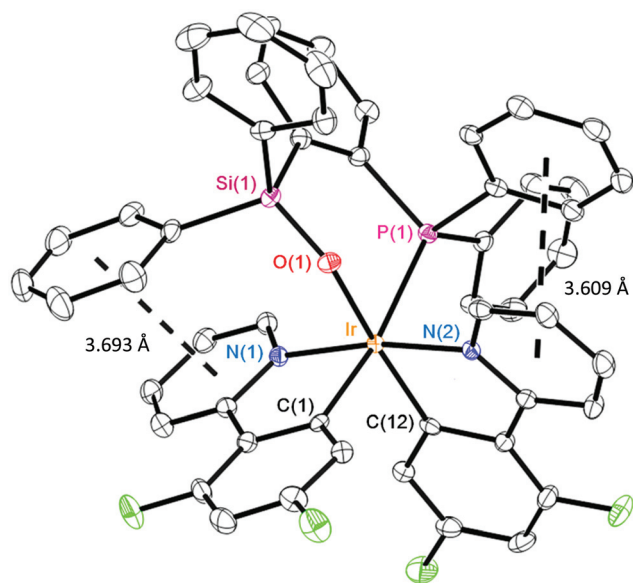


Fig. 1 ORTEP diagram of **3a** with ellipsoids shown at 40% probability level; selected bond distances (Å): Ir–N(1) 2.058(2), Ir–N(2) 2.040(2), Ir–C(1) 2.038(3), Ir–C(12) 1.995(3), Ir–P(1) 2.4045(8), Ir–O(1) 2.126(2); dashed lines show the centroid–centroid contacts between adjacent phenyl substituents.

expected variation of Ir–C distances at the cyclometalate chelates, confirming the generalized structural behavior of this class of Ir(III) metal complexes.⁵¹

Moreover, the X-ray structural analysis also revealed the presence of two sets of intramolecular $\pi\cdots\pi$ stacking interactions (Fig. 1). The first is ascribed to the close contact between one phenyl group of the Ph₂P fragment and the pyridyl group of adjacent dfppy chelate, for which the centroid–centroid contact is calculated to be 3.609 Å. The other is observed between the second pyridyl group of dfppy chelate and the diphenylsilyl substituent, which is documented by a comparable centroid–centroid contact of 3.693 Å. In good agreement with this finding, a large variation of centroid–centroid π – π separation of 3.52–3.74 Å was detected among cationic Ir(III) complexes, for which the π – π stacking interaction was found to be associated with the degree of fluorination at the phenyl pendant of ancillary chelate.⁵²

Photophysical data

The absorption and luminescence spectra of complexes **1–3** in CH₂Cl₂ are depicted in Fig. 2, and their metrical parameters are summarized in Table 1. The strong absorption bands in the UV region with distinct vibronic features are assigned to the spin-allowed $^1\pi\pi^*$ transition of the C^{^N} cyclometalates. The lowest energy absorption with peak wavelengths in the region of 382–466 nm can be ascribed to a spin-allowed metal-to-ligand charge-transfer transition ($^1\text{MLCT}$), while their extinction coefficients at the peak wavelength are in the range of 3000–5000 M^{–1} cm^{–1}. Finally, the weak shoulder that further extends into the longer wavelength region is believed to be associated with the spin-forbidden $^3\pi\pi^*$ and $^3\text{MLCT}$ transitions.

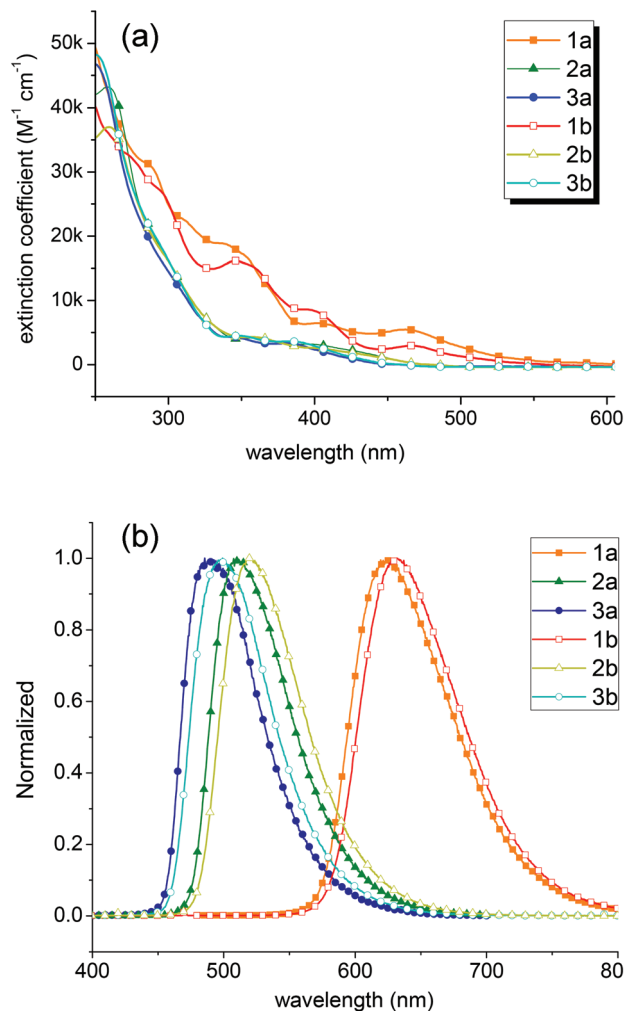


Fig. 2 UV-Vis absorption (a) and normalized emission spectra (b) of the studied Ir(III) metal complexes **1a/1b–3a/3b** in CH₂Cl₂ solution at RT.

Highly intensive luminescence was observed for **1a/1b**, **2a/2b** and **3a/3b** in degassed CH₂Cl₂ with λ_{max} located at 624/632 nm, 510/520 nm and 489/499 nm, respectively, among which the SiPh₂ substituted isomers **a** always showed a much blue-shifted emission *vs.* that of the SiMe₂ substituted counterparts **b** due to the greater electron withdrawing character of the SiPh₂ substituent. Moreover, the entire emission band originating from a triplet state manifold was ascertained by the O₂ quenching rate constant of as high as 1.5–2.0 × 10⁹ M^{–1} s^{–1} for all samples in CH₂Cl₂. The significant overlap of the 0–0 onsets between emission signal and the lowest energy absorption band, in combination with a broad, structureless spectral feature even for the blue-emitting **3a** and **3b**, leads us to conclude that the phosphorescence originates primarily from the $^3\text{MLCT}$ state, together perhaps with a lesser contribution from the $^3\pi\pi^*$ excited states. In comparison to **1a** and **1b** with the piq cyclometalates, complexes **2a** and **2b** and **3a** and **3b** bearing either ppy or dfppy group reveal a ~110 nm and additional ~20 nm hypsochromic shift in the emission peak wavelength, the results of which can qualitatively be

Table 1 Photophysical and electrochemical data of the studied Ir(III) metal complexes in CH₂Cl₂ solution

	UV/Vis λ_{\max}/nm ($10^{-3}\epsilon^a/\text{M}^{-1}\text{cm}^{-1}$)	$\lambda_{\max}^{\text{em}}/\text{nm}$	Φ (%)	$\tau_{\text{obs}}/\mu\text{s}$	$10^{-5}k_{\text{r}}(\text{s}^{-1})$	$10^{-5}k_{\text{nr}}(\text{s}^{-1})$	$E_{1/2}^{\text{ox}}(\Delta E_{\text{p}})^b$	$E_{1/2}^{\text{red}}(\Delta E_{\text{p}})^b$
1a	335 (18), 400 (6.5), 462 (5.5)	624	0.26	1.57	1.63	4.73	0.35 (90)	-2.33 (110), -2.55 (110)
2a	259 (47), 358 (5.0), 394 (3.9)	510	0.73	1.66	4.38	1.64	0.37 (90)	-2.8 (irr)
3a	345 (5.1), 382 (4.0)	489	0.62	0.92	6.79	4.09	0.64 (80)	-2.8 (irr)
1b	347 (18), 395 (9.7), 466 (3.6)	632	0.36	1.36	2.63	4.72	0.33 (110)	-2.34 (130), -2.59 (140)
2b	260 (41), 361 (5.0), 402 (3.2)	520	0.90	1.72	5.23	0.58	0.34 (90)	-2.8 (irr)
3b	350 (5.3), 385 (4.3)	499	0.59	0.66	8.98	6.26	0.59 (90)	-2.7 (irr)

^a The systematic error of the absorption coefficient measurement is $\sim\pm 20\%$. ^b $E_{1/2}$ (V) refers to $[(E_{\text{pa}} + E_{\text{pc}})/2]$ where E_{pa} and E_{pc} are the anodic and cathodic peak potentials referenced to the Fc⁺/Fc couple; $\Delta E_{\text{p}} = |E_{\text{pa}} - E_{\text{pc}}|$ are reported in mV, the reduction experiments were conducted in THF solution; irr indicates irreversible process.

rationalized by a reduction of ligand-centered $\pi\pi^*$ energy gap due to the diminished π -conjugation on the ppy vs. piq cyclometalate, as well as the electron-withdrawing 4,6-difluoro substituents of the dfppy units. This observation is in accordance with the general color-tuning principle of transition-metal based phosphors.^{2,14,53} Table 1 lists the corresponding photophysical data for the studied complexes in degassed CH₂Cl₂ solution at room temperature. The reddest emitting **1a** and **1b** tend to possess the lowest emission quantum yield, which could be attributed to the effect of energy-gap law;⁵⁴ on the other hand, the reduced emission quantum yield for the blue-emitting **3a** and **3b** vs. that of the green-emitting **2a** and **2b** is probably caused by the thermally induced thermal population to the upper-lying metal-centered dd excited state, which led to the faster radiationless deactivation to the ground state, giving the less efficient emission quantum yield.^{55,56} Both of the physical characteristics such as Φ and τ_{obs} are comparable to those of Ir(III) metal phosphors reported in literature.^{53,57–65}

Electrochemistry

The electrochemical behavior of complexes **1–3** was investigated by cyclic voltammetry using ferrocene as the internal standard. The respective redox data are listed in Table 1. During the anodic scan in CH₂Cl₂, all Ir(III) metal complexes exhibited an irreversible oxidation peak in the region of 0.33–0.64 V, which is assigned as the metal-centered oxidation process. Moreover, the anodic potentials showed a systematic trend of **3a/3b** \gg **2a/2b** $>$ **1a/1b**, which is also in agreement with the estimated electron density at the Ir(III) metal center. On the other hand, despite of their large variation in color, the small variation of oxidation potential between the pair of complexes **2a/2b** and **1a/1b** was attributed to the much smaller influence of the overall electron density at the Ir(III) center vs. the π -conjugation of the chelating ligand.

Upon switching to the cathodic sweep in THF, two reversible peaks ranging from -2.33 to -2.59 V were also detected for the red-emitting **1a** and **1b**, while the remainder of green and blue-emitting complexes showed only a single irreversible peak at ca. -2.8 V. Apparently, the extended π -conjugation of the piq chelate would afford the lower lying empty orbital for the incoming electron. In contrast, complexes **2a/2b** and **3a/3b** would afford much more negative reduction potentials due to

the less conjugated pyridyl group present on either ppy or dfppy chelates vs. the isoquinolynyl group of piq chelate.

Electroluminescent devices

To test the applicability of the Ir(III) complexes as emitters in electroluminescence (EL), we selected **3a** and **3b** as the dopants. Selection of dopants was based on the fact that the

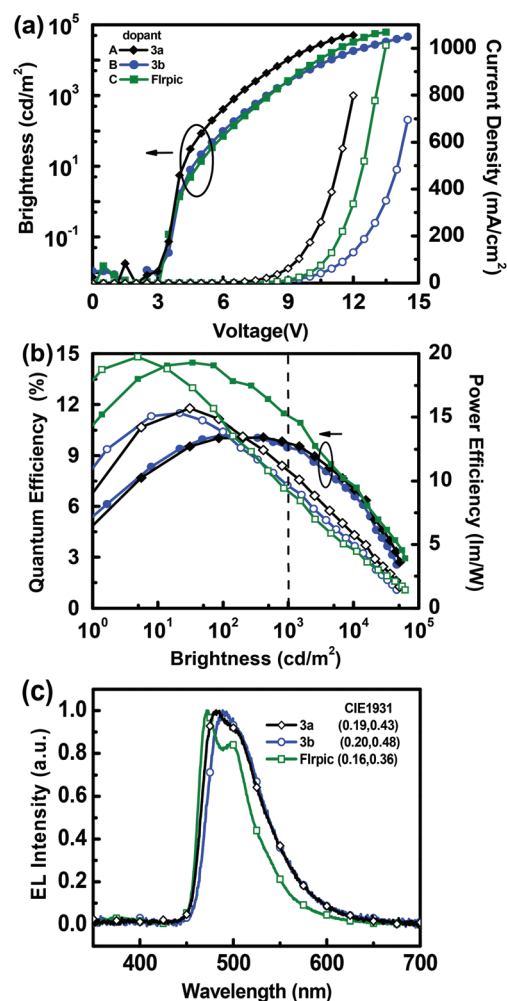


Fig. 3 (a) Current density–voltage–luminance (J – V – L) characteristics. (b) External quantum and power efficiencies as a function of brightness. (c) EL spectra of devices of PhOLEDs with different dopants.

Table 2 EL performances of devices fabricated with blue–green phosphors **3a** and **3b**

	Dopant	V_{on}^b/V	$L_{\text{max}}/\text{cd m}^{-2}$	$I_{\text{max}}/\text{mA cm}^{-2}$	η_{ext} (%)	$\eta_c/\text{cd A}^{-1}$	$\eta_p/\text{lm W}^{-1}$	($V, \%$) ^c at 1000 cd m^{-2}	CIE [x, y]
A ^a	3a	3	50 800 (12.0 V)	800	10.1	23.7	15.7	(6.7, 9.7)	0.19, 0.43
B	3b	3	45 900 (14.5 V)	700	10.2	26.5	15.3	(8, 9.5)	0.20, 0.48
C	Flrpic	3	62 000 (13.5 V)	1010	14.5	30.3	19.7	(8.1, 11.2)	0.16, 0.36

^a The notations A, B and C indicate the devices fabricated with employment of dopants **3a**, **3b** and Flrpic, respectively. ^b Turn-on voltage at which emission became detectable. ^c The values of driving voltage and η_{ext} of device at 1000 cd m^{-2} .

blue–green emitting complexes **3a** and **3b** are the materials with the highest thermal stability upon sublimation and hence give the least amount of tarry material during the evaporation processes. A optimized device consists of the multi-layer architecture: ITO|PEDOT:PSS (30 nm)|TAPC (20 nm)|TCTA (5 nm)|mCP: **3a** or **3b** (10 wt%, 25 nm)|TAZ (50 nm)|LiF (0.5 nm)|Al (100 nm). We used *N,N*-dicarbazolyl-3,5-benzene (mCP) as host material as it possesses a high triplet energy of 2.9 eV and has served as the host for blue PhOLEDs in many reports.⁶⁶ Here, the conducting polymer, poly(ethylene dioxythiophene)/poly(styrene sulfonate) (PEDOT:PSS) is used as the hole-injection and passivation layer, while both 1,1'-bis[4-[*N,N*-di(*p*-tolyl)amino]phenyl]cyclohexane (TAPC)⁶⁷ and 4,4',4'-tri(*N*-carbazolyl)triphenylamine (TCTA)^{68,69} are employed as hole-transport layers, 3-(4-biphenyl-yl)-4-phenyl-5-(4-*tert*-butylphenyl)-1,2,4-triazole (TAZ)⁷⁰ as an electron-transport and hole-blocking layer, LiF as an electron-injection layer and Al as a cathode, respectively. For comparison, the control device C was also fabricated using Flrpic as dopant under the same device structure.

Fig. 3 shows the current density–voltage–brightness (J – V – L) characteristics and efficiency vs. brightness curves for the devices, and the electroluminescence (EL) data are summarized in Table 2. As indicated in Fig. 3a, all of the devices exhibited turn-on voltages of 3 V and the difference in the J – V performances is presumably because of the different emitting dopants that influence the charge carrier transport of EML. The current density and brightness of **3a**-based device A exhibited a maximum brightness (L_{max}) as high as $50\,800 \text{ cd m}^{-2}$ at 12.0 V (800 mA cm^{-2}), which is distinctly higher than that of the **3b**-based device B ($45\,900 \text{ cd m}^{-2}$ at 14.5 V at 700 mA cm^{-2}). The operating voltage at 1000 cd m^{-2} of device A (6.7 V) is slightly lower than that of the device B (8.0 V). In Fig. 3b, **3a**-based device A achieves maximum external quantum efficiency (η_{ext}) of 10.1% corresponding to a current efficiency (η_c) of 23.7 cd A^{-1} and power efficiency (η_p) of 15.7 lm W^{-1} , which are similar to those of the **3b**-based device B (10.2%, 26.5 cd A^{-1} , 15.3 lm W^{-1}). It is worth mentioning that the maximum efficiencies in the devices appeared to occur in the more useful brightness range of 100 – 500 cd m^{-2} , and exhibited low efficiency roll-off at high brightness; the η_{ext} of devices A and B at 1000 cd m^{-2} were 9.7 and 9.5%, respectively. For comparison, device C was also fabricated using Flrpic as emitter under the same device structure, for which the η_{ext} of 14.5% is higher than the device using **3a** or **3b** as dopant. As depicted in Fig. 3c, devices exhibited sky-blue emission with the

corresponding CIE coordinates $x = 0.19, y = 0.43$ for **3a** and $x = 0.20, y = 0.48$ for **3b**, respectively, which are similar to that observed in the PL spectra recorded in dilute solution (Fig. 2). Overall, our device performance data are judged to be moderate, in comparison to the recent documented reports on the blue-emitting PhOLEDs.^{71,72} The reduced performance could be in part attributed by the inherent nature of the silanolate ancillary.

Conclusion

In summary, a series of phosphine-substituted organosilanes were synthesized, which were then utilized as the source for the *in situ* generation of an $\text{P}^{\wedge}\text{SiO}$ ancillary for assembling of Ir(III) based multi-colored phosphors. The transformation from silane to silanolate has been discussed and is associated with metal-catalyzed oxidative hydrolysis. The as-synthesized Ir(III) complexes showed bright luminescence that could be tuned from blue–green to red depending on the cyclometalate chromophores. Although these Ir(III) complexes are stable against moisture during work-up, they tended to exhibit insufficient stability during sublimation at higher temperature. Despite this potential weakness, blue-emitters for PhOLEDs were successfully synthesized, showing the potential for such an ancillary chelate in preparation of new Ir(III) phosphors. Fabrication of PhOLEDs using a solution process, which does not require thermal deposition of emitting layer, is deemed to be more suitable for such type of phosphors toward applications as either displays or lighting applications.

Acknowledgements

This work was gratefully supported by the Hsinchu-Beijing Tsing Hua Collaboration Fund.

References

- X.-H. Zhu, J. Peng, Y. Cao and J. Roncali, *Chem. Soc. Rev.*, 2011, **40**, 3509.
- G. Zhou, W.-Y. Wong and X. Yang, *Chem.–Asian J.*, 2011, **6**, 1706.
- L. Xiao, Z. Chen, B. Qu, J. Luo, S. Kong, Q. Gong and J. Kido, *Adv. Mater.*, 2011, **23**, 926.
- H. Sasabe and J. Kido, *Chem. Mater.*, 2011, **23**, 621.

- 5 A. Chaskar, H.-F. Chen and K.-T. Wong, *Adv. Mater.*, 2011, **23**, 3876.
- 6 Y. Chi and P.-T. Chou, *Chem. Soc. Rev.*, 2010, **39**, 638.
- 7 Y. You and S. Y. Park, *Dalton Trans.*, 2009, 1267.
- 8 J. A. G. Williams, S. Develay, D. L. Rochester and L. Murphy, *Coord. Chem. Rev.*, 2008, **252**, 2596.
- 9 K. A. King, P. J. Spellane and R. J. Watts, *J. Am. Chem. Soc.*, 1985, **107**, 1431.
- 10 C. Adachi, M. A. Baldo, S. R. Forrest and M. E. Thompson, *Appl. Phys. Lett.*, 2000, **77**, 904.
- 11 A. Tsuboyama, H. Iwawaki, M. Furugori, T. Mukaide, J. Kamatani, S. Igawa, T. Moriyama, S. Miura, T. Takiguchi, S. Okada, M. Hoshino and K. Ueno, *J. Am. Chem. Soc.*, 2003, **125**, 12971.
- 12 A. B. Tamayo, B. D. Alleyne, P. I. Djurovich, S. Lamansky, I. Tsyba, N. N. Ho, R. Bau and M. E. Thompson, *J. Am. Chem. Soc.*, 2003, **125**, 7377.
- 13 K. Dedeian, P. I. Djurovich, F. O. Garces, G. Carlson and R. J. Watts, *Inorg. Chem.*, 1991, **30**, 1685.
- 14 F.-M. Hwang, H.-Y. Chen, P.-S. Chen, C.-S. Liu, Y. Chi, C.-F. Shu, F.-I. Wu, P.-T. Chou, S.-M. Peng and G.-H. Lee, *Inorg. Chem.*, 2005, **44**, 1344.
- 15 P.-T. Chou and Y. Chi, *Chem.-Eur. J.*, 2007, **13**, 380.
- 16 T. Tsuzuki and S. Tokito, *Adv. Mater.*, 2007, **19**, 276.
- 17 X. Wei, J. Peng, J. Cheng, M. Xie, Z. Lu, C. Li and Y. Cao, *Adv. Funct. Mater.*, 2007, **17**, 3319.
- 18 G. Zhou, C.-L. Ho, W.-Y. Wong, Q. Wang, D. Ma, L. Wang, Z. Lin, T. B. Marder and A. Beeby, *Adv. Funct. Mater.*, 2008, **18**, 499.
- 19 J. Li, P. I. Djurovich, B. D. Alleyne, I. Tsyba, N. N. Ho, R. Bau and M. E. Thompson, *Polyhedron*, 2004, **23**, 419.
- 20 E. Baranoff, S. Fantacci, F. De Angelis, X. Zhang, R. Scopelliti, M. Gratzel and M. K. Nazeeruddin, *Inorg. Chem.*, 2011, **50**, 451.
- 21 S. Tao, S. L. Lai, C. Wu, T. W. Ng, M. Y. Chan, W. Zhao and X. Zhang, *Org. Electron.*, 2011, **12**, 2061.
- 22 L. Deng, T. Zhang, R. Wang and J. Li, *J. Mater. Chem.*, 2012, **22**, 15910.
- 23 L. Chen, H. You, C. Yang, D. Ma and J. Qin, *Chem. Commun.*, 2007, 1352.
- 24 Y. Liu, K. Ye, Y. Fan, W. Song, Y. Wang and Z. Hou, *Chem. Commun.*, 2009, 3699.
- 25 T. Peng, Y. Yang, Y. Liu, D. Ma, Z. Hou and Y. Wang, *Chem. Commun.*, 2011, **47**, 3150.
- 26 Y. Liu, G. Gahungu, X. Sun, J. Su, X. Qu and Z. Wu, *Dalton Trans.*, 2012, **41**, 7595.
- 27 S.-J. Yeh, M.-F. Wu, C.-T. Chen, Y.-H. Song, Y. Chi, M.-H. Ho, S.-F. Hsu and C. H. Chen, *Adv. Mater.*, 2005, **17**, 285.
- 28 E. Orselli, G. S. Kottas, A. E. Konradsson, P. Coppo, R. Froehlich, L. De Cola, A. van Dijken, M. Buechel and H. Boerner, *Inorg. Chem.*, 2007, **46**, 11082.
- 29 S. Lamansky, P. Djurovich, D. Murphy, F. Abdel-Razzaq, R. Kwong, I. Tsyba, M. Bortz, B. Mui, R. Bau and M. E. Thompson, *Inorg. Chem.*, 2001, **40**, 1704.
- 30 Y.-C. Zhu, L. Zhou, H.-Y. Li, Q.-L. Xu, M.-Y. Teng, Y.-X. Zheng, J.-L. Zuo, H.-J. Zhang and X.-Z. You, *Adv. Mater.*, 2011, **23**, 4041.
- 31 E. Orselli, R. Q. Albuquerque, P. M. Franssen, R. Froehlich, H. M. Janssen and L. De Cola, *J. Mater. Chem.*, 2008, **18**, 4579.
- 32 S.-C. Lo, R. E. Harding, C. P. Shipley, S. G. Stevenson, P. L. Burn and I. D. W. Samuel, *J. Am. Chem. Soc.*, 2009, **131**, 16681.
- 33 Y.-C. Chiu, J.-Y. Hung, Y. Chi, C.-C. Chen, C.-H. Chang, C.-C. Wu, Y.-M. Cheng, Y.-C. Yu, G.-H. Lee and P.-T. Chou, *Adv. Mater.*, 2009, **21**, 2221.
- 34 C.-H. Lin, Y. Chi, M.-W. Chung, Y.-J. Chen, K.-W. Wang, G.-H. Lee, P.-T. Chou, W.-Y. Hung and H.-C. Chiu, *Dalton Trans.*, 2011, **40**, 1132.
- 35 J.-Y. Hung, C.-H. Lin, Y. Chi, M.-W. Chung, Y.-J. Chen, G.-H. Lee, P.-T. Chou, C.-C. Chen and C.-C. Wu, *J. Mater. Chem.*, 2010, **20**, 7682.
- 36 B.-S. Du, C.-H. Lin, Y. Chi, J.-Y. Hung, M.-W. Chung, T.-Y. Lin, G.-H. Lee, K.-T. Wong, P.-T. Chou, W.-Y. Hung and H.-C. Chiu, *Inorg. Chem.*, 2010, **49**, 8713.
- 37 J.-Y. Hung, Y. Chi, I.-H. Pai, Y.-M. Cheng, Y.-C. Yu, G.-H. Lee, P.-T. Chou, K.-T. Wong, C.-C. Chen and C.-C. Wu, *Dalton Trans.*, 2009, 6472.
- 38 Y.-C. Chiu, Y. Chi, J.-Y. Hung, Y.-M. Cheng, Y.-C. Yu, M.-W. Chung, G.-H. Lee, P.-T. Chou, C.-C. Chen, C.-C. Wu and H.-Y. Hsieh, *ACS Appl. Mater. Interfaces*, 2009, **1**, 433.
- 39 K. S. Yook and J. Y. Lee, *Adv. Mater.*, 2012, **24**, 3169.
- 40 Y.-H. Song, Y.-C. Chiu, Y. Chi, Y.-M. Cheng, C.-H. Lai, P.-T. Chou, K.-T. Wong, M.-H. Tsai and C.-C. Wu, *Chem.-Eur. J.*, 2008, **14**, 5423.
- 41 C.-H. Lin, Y.-C. Chiu, Y. Chi, Y.-T. Tao, L.-S. Liao, M.-R. Tseng and G.-H. Lee, *Organometallics*, 2012, **31**, 4349.
- 42 M. Safa, M. C. Jennings and R. J. Puddephatt, *Organometallics*, 2012, **31**, 3539.
- 43 Y. Lee, D. Seomoon, S. Kim, H. Han, S. Chang and P. H. Lee, *J. Org. Chem.*, 2004, **69**, 1741.
- 44 M. K. Hays and R. Eisenberg, *Inorg. Chem.*, 1991, **30**, 2623.
- 45 S. R. Klei, T. Don Tilley and R. G. Bergman, *Organometallics*, 2002, **21**, 3376.
- 46 M. Aizenberg and D. Milstein, *Organometallics*, 1996, **15**, 3317.
- 47 B. Marciniak, I. Kownacki and M. Kubicki, *Organometallics*, 2002, **21**, 3263.
- 48 Y. You, J. Seo, S. H. Kim, K. S. Kim, T. K. Ahn, D. Kim and S. Y. Park, *Inorg. Chem.*, 2008, **47**, 1476.
- 49 Y. Liu, M.-Y. Li, Q. Zhao, H.-Z. Wu, K.-W. Huang and F.-Y. Li, *Inorg. Chem.*, 2011, **50**, 5969.
- 50 E. Baranoff, B. F. E. Curchod, F. Monti, F. Steimer, G. Accorsi, I. Tavernelli, U. Rothlisberger, R. Scopelliti, M. Gratzel and M. K. Nazeeruddin, *Inorg. Chem.*, 2012, **51**, 799.
- 51 T.-C. Lee, C.-F. Chang, Y.-C. Chiu, Y. Chi, T.-Y. Chan, Y.-M. Cheng, C.-H. Lai, P.-T. Chou, G.-H. Lee, C.-H. Chien, C.-F. Shu and J. Leonhardt, *Chem.-Asian J.*, 2009, **4**, 742.

- 52 L. He, D. Ma, L. Duan, Y. Wei, J. Qiao, D. Zhang, G. Dong, L. Wang and Y. Qiu, *Inorg. Chem.*, 2012, **51**, 4502.
- 53 M. Tavasli, T. N. Moore, Y. Zheng, M. R. Bryce, M. A. Fox, G. C. Griffiths, V. Jankus, H. A. Al-Attar and A. P. Monkman, *J. Mater. Chem.*, 2012, **22**, 6419.
- 54 A. Vlcek Jr, *Top. Organomet. Chem.*, 2010, **29**, 73.
- 55 R. E. Harding, S.-C. Lo, P. L. Burn and I. D. W. Samuel, *Org. Electron.*, 2008, **9**, 377.
- 56 P.-T. Chou, Y. Chi, M.-W. Chung and C.-C. Lin, *Coord. Chem. Rev.*, 2011, **255**, 2653.
- 57 M. Zhu, Y. Li, C. g. Li, C. Zhong, C. Yang, H. Wu, J. Qin and Y. Cao, *J. Mater. Chem.*, 2012, **22**, 11128.
- 58 Y. Zhou, W. Li, Y. Liu, L. Zeng, W. Su and M. Zhou, *Dalton Trans.*, 2012, **41**, 9373.
- 59 X. Yang, Y. Zhao, X. Zhang, R. Li, J. Dang, Y. Li, G. Zhou, Z. Wu, D. Ma, W.-Y. Wong, X. Zhao, A. Ren, L. Wang and X. Hou, *J. Mater. Chem.*, 2012, **22**, 7136.
- 60 M. Song, J. S. Park, Y.-S. Gal, S. Kang, J. Y. Lee, J. W. Lee and S.-H. Jin, *J. Phys. Chem. C*, 2012, **116**, 7526.
- 61 V. K. Rai, M. Nishiura, M. Takimoto, S. Zhao, Y. Liu and Z. Hou, *Inorg. Chem.*, 2012, **51**, 822.
- 62 G. St-Pierre, S. Ladouceur, D. Fortin and E. Zysman-Colman, *Dalton Trans.*, 2011, **40**, 11726.
- 63 A. Santoro, A. M. Prokhorov, V. N. Kozhevnikov, A. C. Whitwood, B. Donnio, J. A. G. Williams and D. W. Bruce, *J. Am. Chem. Soc.*, 2011, **133**, 5248.
- 64 M. Li, H. Zeng, Y. Meng, H. Sun, S. Liu, Z. Lu, Y. Huang and X. Pu, *Dalton Trans.*, 2011, **40**, 7153.
- 65 S. Ladouceur, D. Fortin and E. Zysman-Colman, *Inorg. Chem.*, 2011, **50**, 11514.
- 66 R. J. Holmes, S. R. Forrest, Y.-J. Tung, R. C. Kwong, J. J. Brown, S. Garon and M. E. Thompson, *Appl. Phys. Lett.*, 2003, **82**, 2422.
- 67 K. Goushi, R. Kwong, J. J. Brown, H. Sasabe and C. Adachi, *J. Appl. Phys.*, 2004, **95**, 7798.
- 68 S.-J. Su, E. Gonmori, H. Sasabe and J. Kido, *Adv. Mater.*, 2008, **20**, 4189.
- 69 Y.-Y. Lyu, J. Kwak, W. S. Jeon, Y. Byun, H. S. Lee, D. Kim, C. Lee and K. Char, *Adv. Funct. Mater.*, 2009, **19**, 420.
- 70 Q. Wang, J. Ding, D. Ma, Y. Cheng, L. Wang, X. Jing and F. Wang, *Adv. Funct. Mater.*, 2009, **19**, 84.
- 71 H. Sasabe, N. Toyota, H. Nakanishi, T. Ishizaka, Y.-J. Pu and J. Kido, *Adv. Mater.*, 2012, **24**, 3212.
- 72 J.-K. Bin, N.-S. Cho and J.-I. Hong, *Adv. Mater.*, 2012, **24**, 2911.